

International Journal of Modern Physics E  
 © World Scientific Publishing Company

## TERMINATING STATES AS A UNIQUE LABORATORY FOR TESTING NUCLEAR ENERGY DENSITY FUNCTIONAL

M. ZALEWSKI\*

*Institute of Theoretical Physics, University of Warsaw,  
 ul. Hoża 69, 00-681 Warsaw, Poland*

W. SATULA†

*Institute of Theoretical Physics, University of Warsaw,  
 ul. Hoża 69, 00-681 Warsaw, Poland,*

Received (received date )

Revised (revised date )

Systematic calculations of favored signature maximum-spin  $I_{max}$  and unfavored signature  $I_{max} - 1$  terminating states for  $[f_{7/2}^n]$  and  $[d_{3/2}^{-1} f_{7/2}^{n+1}]$  configurations ( $n$  denotes number of valence particles) in  $A \sim 44$  mass region are presented. Following the result of Zduńczuk *et al.*, Phys. Rev. C**71** (2005) 024305 the calculations are performed using Skyrme energy density functional with empirical Landau parameters and slightly reduced spin-orbit strength. The aim is to identify and phenomenologically restore rotational symmetry broken by the Skyrme-Hartree-Fock solutions. In particular, it is shown that correlation energy due to symmetry restoration is absolutely crucial in order to reproduce energy splitting  $E(I_{max}) - E(I_{max} - 1)$  in  $[f_{7/2}^n]$  configurations but is relatively less important for  $[d_{3/2}^{-1} f_{7/2}^{n+1}]$  configurations.

### 1. Introduction

Structure of heavy nuclei may be described using two major theoretical approaches: the nuclear shell-model<sup>1</sup> (SM) and the nuclear density functional theory<sup>2</sup> (DFT). The main advantage of SM is proper treatment of many-body correlations among limited number of valence particles. The resulting wave functions are eigenstates to symmetry invariants of the effective Hamiltonian. In the language of DFT, nucleus is treated as  $A$ -body composite object described by one-body densities and currents. According to the Hohenberg-Kohn-Sham (HKS) theorem<sup>3</sup>, this method is formally exact. However, since the HKS theorem does not provide any method of constructing such an exact functional standard procedures employed in nuclear physics attempt to construct the functional in a systematic way guided by basic

\*zalewiak@fuw.edu.pl

†satula@fuw.edu.pl

2 *M. Zalewski, W. Satuła*

symmetry requirements<sup>4</sup>. A particular case of the nuclear EDF is the functional inspired by well studied Skyrme model<sup>2,5,6</sup> (S-EDF) which, in the isoscalar-isovector  $t = 0, 1$  representation, takes the following form:

$$\mathcal{E}^{Skyrme} = \sum_{t=0,1} \int d^3\mathbf{r} \left[ \mathcal{H}_t^{(TE)}(\mathbf{r}) + \mathcal{H}_t^{(TO)}(\mathbf{r}) \right], \quad (1)$$

where

$$\mathcal{H}_t^{(TE)}(\mathbf{r}) = C_t^\rho \rho_t^2 + C_t^{\Delta\rho} \rho_t \Delta \rho_t + C_t^\tau \rho_t \tau_t + C_t^J J_t^2 + C_t^{\nabla J} \rho_t \nabla \cdot \mathbf{J}_t, \quad (2)$$

$$\mathcal{H}_t^{(TO)}(\mathbf{r}) = C_t^s s_t^2 + C_t^{\Delta s} s_t \Delta s_t + C_t^T \mathbf{s}_t \cdot \mathbf{T}_t + C_t^j j_t^2 + C_t^{\nabla j} \mathbf{s}_t \cdot (\nabla \times \mathbf{j}_t). \quad (3)$$

The functional  $\mathcal{H}$  is uniquely expressed as a bilinear form of time-even (TE)  $\rho, \tau, J$  and time-odd (TO)  $\mathbf{s}, \mathbf{T}, \mathbf{j}$  local densities, currents, and by their derivatives. Exact expressions linking auxiliary Skyrme parameters  $x_i, t_i$ ,  $i = 0, 1, 2, 3$  and  $W, \alpha$  with coupling constants  $C$  can be found, for example, in Ref.<sup>2</sup>.

The coupling constants of the S-EDF (or Skyrme force (SF)) are adjusted to global properties of nuclear matter and to selected experimental observables in order to account for basic nuclear structure properties. Since there exist a multitude of observables and no real consensus about which of these are to be selected in a unique manner, there exist a multitude of different SF parameterizations. One of the basic problems in adjusting the force parameters is related to the fact that the single-particle (SP) states, that are so crucial for high accuracy calculations, are in general coupled to collective motion and therefore difficult to determine. In this context, any dataset representing SP motion is an invaluable source of information that can be used for a rigorous test and subsequent fine-tuning of the parameters.

Our long standing experience tells us that terminating states which are maximum-spin states within given SP configuration are one of the best examples of unperturbed SP motion<sup>7,8</sup>. This conclusion was recently confirmed by a comparative study between state of the art SM and Skyrme-Hartree-Fock calculation<sup>9</sup> performed for maximum spin  $I_{max}$  states terminating within  $f_{7/2}^n$  and  $d_{3/2}^{-1}f_{7/2}^{n+1}$  configurations in  $N>Z$ ,  $A\sim 44$  nuclei. Indeed, for these cases the energy difference

$$\Delta E = E[d_{3/2}^{-1}f_{7/2}^{n+1}]_{I_{max}} - E[f_{7/2}^n]_{I_{max}}, \quad (4)$$

calculated using Skyrme-Hartree-Fock (SHF) approach with modified spin-fields and spin-orbit (SO) strength<sup>10</sup> follows very closely the results of SM calculations. This study revealed simultaneously that in  $N=Z$  nuclei the extreme SP picture breaks down due to spontaneous breaking of isobaric symmetry.

The aim of this work is to explore the structural simplicity of maximum-spin  $I_{max}$  (favored signature) as well as for  $I_{max} - 1$  (unfavored signature) terminating states in order to further constrain parameters of the S-LEDF as well as in order to identify, quantitatively evaluate and subsequently restore in a phenomenological way broken symmetries inherently obscuring the SHF treatment. In particular, we will show that the energy difference of Eq. (4) between  $I_{max}$  configurations

$p_{1/2}^{-1}d_{5/2}^{n+1}$  and  $d_{5/2}^n$  in  $A \sim 16$  mass region and between  $I_{max}$  configurations  $f_{5/2}^{-1}g_{9/2}^{n+1}$  and  $g_{9/2}^n$  in  $A \sim 80$  mass region follows closely the trend found in  $A \sim 44$  mass region in Refs. 10 with respect to the isoscalar effective mass scaled isoscalar strength of SO term and that this result nicely correlates with simple Nilsson model predictions concerning  $N=Z=8$  and  $N=Z=40$  magic gaps. In the second part we will demonstrate that unfavored signature  $I_{max} - 1$  terminating states in  $A \sim 44$  mass region manifestly violate rotational invariance. However, unlike in most other cases where the spontaneous breaking of rotational symmetry (SSB) leads to the occurrence of deformation what allows to incorporate substantial fraction of many-body correlations into a single deformed Slater determinant, see Ref. 8 and refs. quoted therein, the effect discussed here occurs at quasi-spherical shape. It appears that there is a fundamental difference between these two situations. In deformed nuclei the SSB mechanism works *constructively*. The violated symmetry can be subsequently approximately restored within independent particle model based on cranking approximation what leads naturally to emergence of collective rotational states. In the case of  $I_{max} - 1$  terminating states the SSB mechanism works *destructively* and one need to go beyond mean-field and perform configuration mixing calculations to restore the symmetry. However, since the number of participating (dominant) configurations is very limited such configuration mixing can be performed analytically, as shown in detail in Sect. 3.

## 2. Isoscalar spin-orbit strength

In Refs. 10 it was shown that the set of terminating states in  $N \neq Z$ ,  $A \sim 44$  mass region provides reliable constraints on time-odd fields and the strength of isoscalar SO interaction of the S-EDF. In particular, it was demonstrated that constraining coupling constants of time odd spin-fields to the empirical spin-isospin Landau parameters leads to unification of predictions for  $\Delta E$  of Eq. (4) for such different Skyrme parameterizations like SLy4 and SLy5<sup>11</sup>, SkO<sup>12</sup>, SIII<sup>13</sup>, and SkXc<sup>14</sup> with mean deviation between calculated and experimental values  $\overline{\Delta E} \sim 500$  keV i.e. at the level of  $\sim 10\%$ . Let us stress that our high-spin estimate of Landau parameters is fairly consistent with the data extracted based on completely different experimental input like giant resonances, beta decays, or moments of inertia<sup>15,16</sup>.

The remaining mean discrepancy  $\overline{\Delta E} \equiv \overline{\Delta E}_{exp} - \overline{\Delta E}_{th}$  between theory and experiment can be further reduced by slightly reducing SO strength. Indeed, the quantity  $\Delta E$  of Eq. (4) is governed by the size of  $N = Z = 20$  magic gap  $\Delta e_{20}$  which, in turn, strongly depends on the SO strength. It can be nicely demonstrated within the spherical Nilsson Hamiltonian<sup>17</sup> where:

$$\Delta e_{20} = \hbar\omega_0(1 - 6\kappa - 2\kappa\mu). \quad (5)$$

For light nuclei  $\mu \sim 0$  i.e. flat bottom and surface effect do not play important role. The width of the potential well  $\hbar\omega_0$  determines global energy scale in low energy nuclear physics. It is rather well constrained by data and even small variations

can spoil in general good agreement between theory and experiment, especially in heavy nuclei. Hence, the SO term  $\kappa$  plays indeed a dominant role in magnitude of the magic gap  $\Delta e_{20}$ .

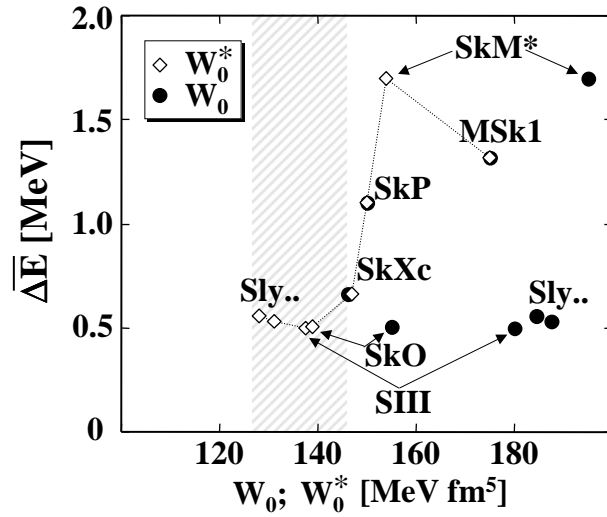


Fig. 1. Mean value  $\overline{\Delta E}$  as a function of the isoscalar strength  $W_0^*$  (filled diamonds) and  $W_0$  (open circles) for different parameterizations of the SF. See text for further discussion. Taken from Ref. 10.

In Refs. 10 it was shown, that  $\overline{\Delta E}$  in  $A \sim 44$  nicely correlates with isoscalar SO strength. However, due to non-local momentum dependent terms, such a correlation cannot be done at the level of bare SO strength  $W_0$ , see black dots in Fig. 2, but must be performed at the level of the so called asymptotically equivalent representation:

$$\tilde{\phi}_i(\vec{r}) = \sqrt{\frac{m}{m^*(\vec{r})}} \phi_i(\vec{r}). \quad (6)$$

In this representation free particles in the infinity  $r \rightarrow \infty$  acquire not effective  $m^*$  but bare mass  $m$  while the SO potential takes the form:

$$V_{LS}(q, r) \approx \frac{m^*(\vec{r})}{m} \left\{ W_0 \frac{1}{r} \rho'_0(r) \pm W_1 \frac{1}{r} \rho'_1(r) \right\} \vec{l} \cdot \vec{s}. \quad (7)$$

Note, that the true SO strength felt by a nucleon is  $W_0^* \equiv \frac{m^*}{m} W_0$  and not  $W_0$ . The correlation between the effective-mass-scaled isoscalar strength is  $W_0^*$  and  $\overline{\Delta E}$  is now evident, see diamonds in Fig. 2. All forces giving similar  $\overline{\Delta E}$  including SLy4, Sly5, SIII, SkO and SkXc have also similar  $W_0^*$  ( $\sim 135 \pm 10$  MeV fm $^5$ ). For SkP<sup>18</sup>, MSk1<sup>19</sup> or SkM\*<sup>20</sup> which give unacceptably large  $\overline{\Delta E}$ ,  $W_0^*$  is also considerably larger.

To further investigate correlation between  $\overline{\Delta E}$  and the SO strength  $W_0^*$  we have performed similar calculations for terminating states  $\Delta E = E([p_{1/2}^{-1} d_{5/2}^{n+1}]_{I_{max}}) -$

Terminating states as a unique laboratory for testing nuclear energy density functional 5

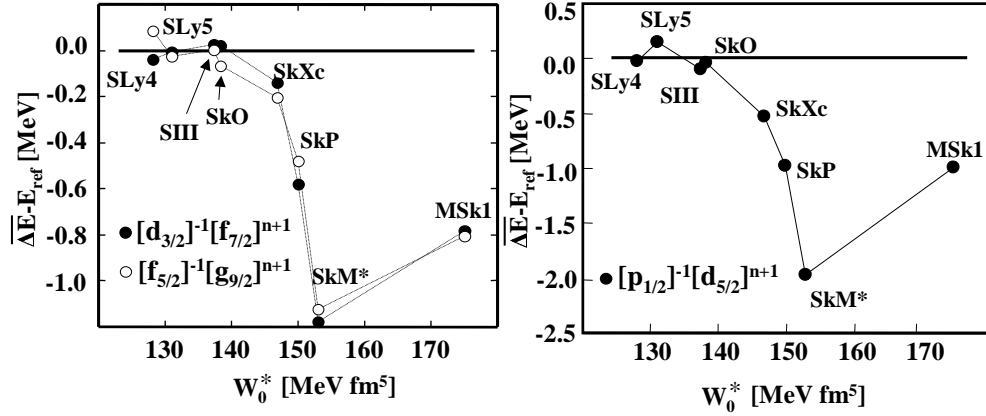


Fig. 2. Left figure shows mean value of  $\overline{\Delta E} - E_{ref}$  in  $A \sim 44$  nuclei in comparison to analogical quantity calculated for  $\Delta E = E([f_{5/2}^{-1}g_{9/2}^{n+1}]) - E([g_{9/2}^n])$  configurations in  $A \sim 80$  nuclei. Right figure shows  $\overline{\Delta E} - E_{ref}$  calculated for  $\Delta E = E([p_{1/2}^{-1}d_{5/2}^{n+1}]) - E([d_{5/2}^n])$  configurations in  $A \sim 16$  nuclei. See text for further details.

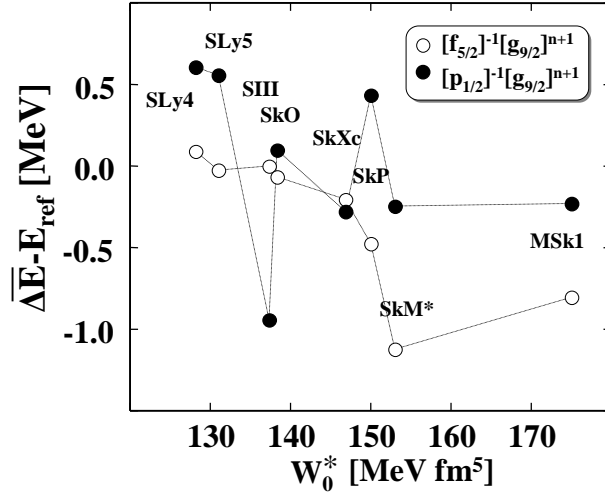


Fig. 3. Comparison of  $\overline{\Delta E} - E_{ref}$  for two possible particle-hole excitations  $[f_{5/2}^{-1}g_{9/2}^{n+1}]$  and  $[p_{1/2}^{-1}g_{9/2}^{n+1}]$  through the magic gap 40.

$E([d_{5/2}^n]_{I_{max}})$  in  $A \sim 16$  mass region and for two different terminating configurations  $\Delta E = E([f_{5/2}^{-1}g_{9/2}^{n+1}]_{I_{max}}) - E([g_{9/2}^n]_{I_{max}})$  and  $\Delta E = E([p_{1/2}^{-1}g_{9/2}^{n+1}]_{I_{max}}) - E([g_{9/2}^n]_{I_{max}})$  in  $A \sim 80$  mass region. The results are depicted in Figs. 2 and 3. Since there is no data for terminating states in these nuclei we compare purely theoretical trends by showing mean value  $\overline{\Delta E} - E_{ref}$  (averaging over different  $N \neq Z$  nuclei) where  $E_{ref}$  denotes mean value of  $\overline{\Delta E}$  calculated using SkO, SIII and Sly4 forces

i.e. those which perform best in  $A \sim 44$  region.

Note, that dependence of  $\overline{\Delta E} - E_{ref}$  on  $W_0^*$  for  $[p_{1/2}^{-1}d_{5/2}^{n+1}]$  and  $[f_{5/2}^{-1}g_{9/2}^{n+1}]$  configurations is very similar to each other and to  $A \sim 44$  case, as shown in Fig. 2. For  $[p_{1/2}^{-1}g_{9/2}^{n+1}]$  states one observes completely different pattern, see Fig. 3. The reason for that becomes clear when one looks at the hierarchy of different contributions to the corresponding energy gaps emerging within Nilsson model:

$$\Delta e_{N=Z=8}^{(d_{5/2}-p_{1/2})} = \hbar\omega_0(1 - 4\kappa), \quad (8)$$

$$\Delta e_{N=Z=20}^{(f_{7/2}-d_{3/2})} = \hbar\omega_0(1 - 6\kappa - 2\kappa\mu), \quad (9)$$

$$\Delta e_{N=Z=40}^{(g_{9/2}-f_{5/2})} = \hbar\omega_0(1 - 8\kappa - 3\kappa\mu), \quad (10)$$

$$\Delta e_{N=Z=40}^{(g_{9/2}-p_{1/2})} = \hbar\omega_0(1 - 6\kappa - 13\kappa\mu). \quad (11)$$

The value of  $\mu$  vary from zero in light nuclei where the surface and flat bottom effects are small to the pseudo-spin limit  $\mu \sim 1/2$  in heavy-nuclei. In (8), (9) and (10) contribution to  $\Delta e$  from flat bottom and surface effect is small in comparison with contribution from SO interaction. The ratio of these two terms (assuming  $\mu = 1/2$ ) for (9) and (10) cases is equal:

$$\frac{\mu}{3} \approx \frac{3\mu}{8} \approx 0.17, \quad (12)$$

and for (8) it is equal zero. In case of  $ph$  excitation from  $p_{1/2}$  to  $g_{9/2}$  sub-shell this ratio is:

$$\frac{13\mu}{6} \approx 1, \quad (13)$$

and one may anticipate qualitative change in physical scenario what indeed takes place as shown in Fig. 3.

### 3. $I_{max} - 1$ states

Unfavored signature  $[f_{7/2}^n]_{I_{max}-1}$  terminating states can be obtained within mean-field theory by changing either the signature of valence neutron or the signature of valence proton. These two independent Slater determinants will be labeled  $|\nu\rangle$  and  $|\pi\rangle$ , respectively. Energy difference, between these states and  $I_{max}$  solution calculated using modified SkO force is shown in the left hand part of Fig. 4. Note that the SHF values are in complete disagreement both with experimental data and SM results. Similar result holds for SLy4 force, see Ref. 21.

The major source of disagreement is related to spontaneous violation of rotational symmetry by these quasi-spherical SHF solutions. Indeed, simple  $m$ -scheme counting shows that both  $I_{max}$  and  $I_{max} - 1$  representations are single-folded within the  $f_{7/2}^n$  Hilbert space irrespective of number of valence particles  $n$ . The SHF solutions are eigenstates of an angular moment projection with  $K = I_{max} - 1$ . Hence, they are mixtures of "spurious"  $|I_{max}, I_{max} - 1\rangle$  and *physical*  $|I_{max} - 1, I_{max} - 1\rangle$  states:

$$|I_{max}, I_{max} - 1\rangle = a|\nu\rangle + b|\pi\rangle, \quad (14)$$

$$|I_{max} - 1, I_{max} - 1\rangle = -b|\nu\rangle + a|\pi\rangle. \quad (15)$$

The symmetry restoration is therefore limited to a simple  $2 \times 2$  mixing problem:

$$\begin{pmatrix} e_1 & V \\ V & e_2 \end{pmatrix} \begin{pmatrix} a \\ b \end{pmatrix} = \lambda \begin{pmatrix} a \\ b \end{pmatrix}. \quad (16)$$

where  $e_1 \equiv E(|\nu\rangle) - E(I_{max})$  and  $e_2 \equiv E(|\pi\rangle) - E(I_{max})$ . The problem can be solved analytically in two different ways. The first method (A) determines  $V$  based on strict requirement that "spurious" solution should be placed at zero energy  $\lambda_1 \equiv 0$ . This corresponds to  $V = \sqrt{e_1 e_2}$  and  $\lambda_2 = e_1 + e_2$ . This is energy of physical  $I_{max} - 1$  state relative to energy of  $I_{max}$  state. The results of this procedure for the SkO-SHF calculations are shown in the right hand side of Fig. 4 (black triangles).

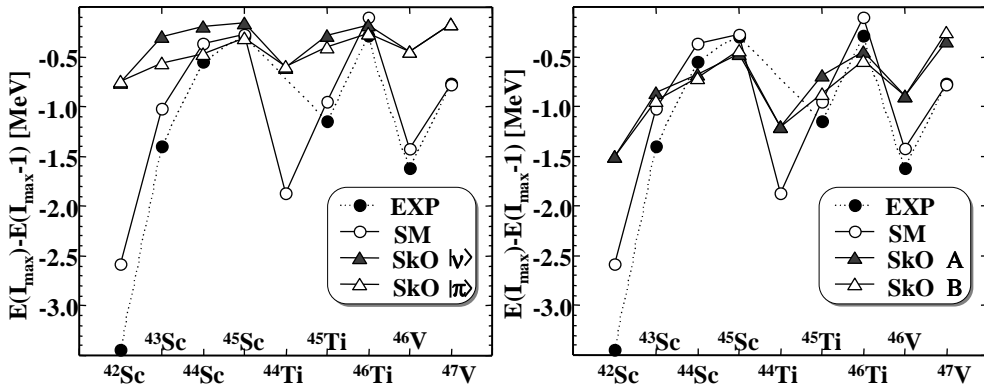


Fig. 4. Energy difference between  $I_{max}$  and  $I_{max} - 1$  states for  $f_{7/2}^n$  configuration. Left panel shows the SkO-SHF solutions  $|\pi\rangle$  and  $|\nu\rangle$  which break rotational symmetry. Right panel show the effect of symmetry restoration according to the methods A and B, respectively. In both cases results are compared with experimental data (dots) and the SM calculations (circles).

The method B uses values of  $a$  and  $b$  coefficients calculated by acting on  $|I_{max}, I_{max}\rangle$  state with  $\hat{I}_-$  operator, see Ref. 21 for details. For example, in  $^{43}\text{Sc}$  we obtain:

$$\hat{I}_-|I_{max}, I_{max}\rangle = |I_{max}, I_{max} - 1\rangle = 2\sqrt{3}|\pi\rangle + \sqrt{7}|\nu\rangle. \quad (17)$$

Knowing  $a$  and  $b$  one may find from (16) the value of interaction  $V$  as well as energies of "spurious" and *physical* solutions  $\lambda_1$  and  $\lambda_2$ :

$$V = \frac{r(e_1 - e_2)}{1 - r^2}, \quad (18)$$

$$\lambda_1 = \frac{e_1 - r^2 e_2}{1 - r^2}, \quad (19)$$

$$\lambda_2 = \frac{e_2 - r^2 e_1}{1 - r^2}, \quad (20)$$

where  $r \equiv b/a$ . Physical solution  $\lambda_2$  is shown the right hand side panel of Fig. 4. Note, that in this case the energy,  $\lambda_1$ , of "spurious" state is not equal zero, but for SkO force it doesn't exceed  $\pm 0.1$  MeV (with exception of  $^{45}\text{Ti}$ ). Note also that method B doesn't work for  $N = Z$  nuclei where  $r = 1$ . It is clearly seen from Fig 4 that our simple symmetry restoring schemes provide very accurate results. More detailed discussion concerning this issue including results for Sly4 force can be found in Ref. 21.

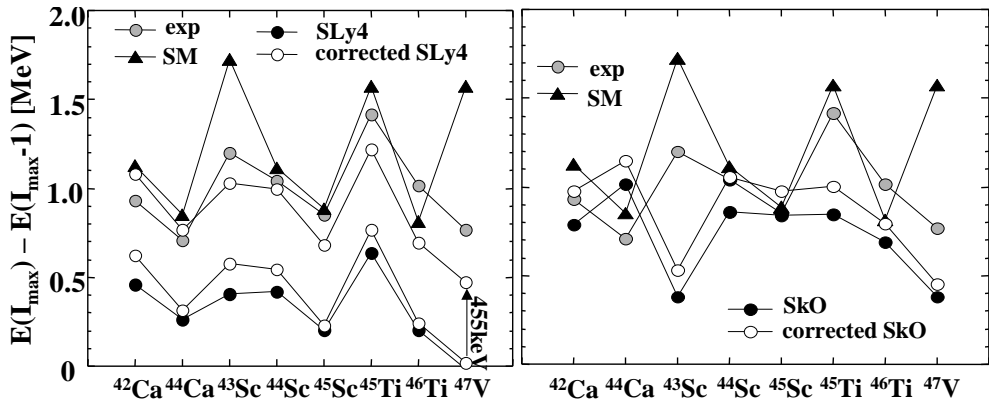


Fig. 5. Energy difference between  $I_{max}$  and the lowest  $I_{max} - 1$  terminating states for  $d_{3/2}^{-1} f_{7/2}^{n+1}$  configuration. Triangles and grey dots denote SM results and experimental data respectively. Black dots represent bare SHF solutions. Circles represent symmetry restored SHF results according to the method A. Left (right) panel illustrates the SLy4-SHF (SkO-SHF) results, respectively. In order to facilitate comparison of isotopic and isotonic dependence of the Sly4 results we include additional curve showing symmetry restored SLy4-SHF solution shifted arbitrarily by 455 keV. The method B, which is not shown for the reasons of clarity, gives larger correction than the method A by  $\sim 100$  keV for both Sly4 and SkO forces.

For  $d_{3/2}^{-1} f_{7/2}^{n+1}$  configuration there are three possibilities of creating  $I_{max} - 1$  states at the mean-field level. One may change the signature of either proton or neutron in  $f_{7/2}$  sub-shell. These states will be labeled as  $|\pi\rangle$  and  $|\nu\rangle$ , respectively. Alternatively, one may change the signature of the proton in  $d_{3/2}$  sub-shell. This Slater determinant will be denoted as  $|\bar{\pi}\rangle$ . Simple  $M$ -scheme counting method shows that our Hilbert space contains two-fold  $I_{max} - 1$  representation. Hence, to restore broken symmetry we have to deal here with  $3 \times 3$  eigen-problem having two physical and one "spurious"  $|I_{max}, I_{max}-1\rangle$  solutions. The most general mixing Hamiltonian matrix can in this case be written as:

$$\begin{pmatrix} e_1 & V_{12} & V_{13}^* \\ V_{12}^* & e_2 & V_{23} \\ V_{13} & V_{23}^* & e_2 \end{pmatrix} \begin{pmatrix} a \\ b \\ c \end{pmatrix} = \lambda \begin{pmatrix} a \\ b \\ c \end{pmatrix}, \quad (21)$$

where  $e_i \equiv E[i] - E[I_{max}]$ , and  $i = |\pi\rangle, |\nu\rangle, |\bar{\pi}\rangle$ . Two different methods of restoring symmetry (called A and B) are proposed below. In both methods the energy of

"spurious" solution is rigorously set to zero. The method A assumes additionally real interaction and precise knowledge of mixing coefficients  $a$ ,  $b$  and  $c$ . The values of  $a$ ,  $b$  and  $c$  are calculated again by using simple angular momentum algebra, in particular by applying  $\hat{I}_-$  to  $|I_{max}, I_{max}\rangle$  reference state, see <sup>21</sup> for details. Method B admits complex interaction and sets no further constraints on  $a$ ,  $b$  and  $c$  coefficients.

In both cases the problem can be solved analytically. Method A gives:

$$\begin{aligned} V_{12} &= \frac{-e_1 a^2 - e_2 b^2 + e_3 c^2}{2ab}, \\ V_{13} &= \frac{-e_1 a^2 + e_2 b^2 - e_3 c^2}{2ac}, \\ V_{23} &= \frac{e_1 a^2 - e_2 b^2 - e_3 c^2}{2bc}, \end{aligned} \quad (22)$$

while in method B we obtain:

$$V_{12} = \sqrt{e_1 e_2}, \quad V_{13} = \sqrt{e_1 e_3}, \quad V_{23} = \sqrt{e_2 e_3}, \quad (23)$$

if  $e_1, e_2, e_3$  are of the same sign or:

$$V_{12} = i\sqrt{-e_1 e_2}, \quad V_{13} = -i\sqrt{-e_1 e_3}, \quad V_{23} = \sqrt{e_2 e_3}, \quad (24)$$

for  $e_1 < 0$  and  $e_2, e_3 > 0$ . Other possibilities are analogous. Knowing the values of interaction one may find the energies of physical  $I_{max} - 1$  states. They are equal:

$$\lambda_{\pm} = \frac{1}{2} (\Sigma \pm \sqrt{\Delta}) \quad (25)$$

where

$$\begin{aligned} \Delta &= \Sigma^2 - 4Z, \\ \Sigma &= e_1 + e_2 + e_3, \\ Z &= e_1 e_2 + e_1 e_3 + e_2 e_3 - |V_{12}|^2 - |V_{13}|^2 - |V_{23}|^2. \end{aligned}$$

The results for the lowest  $I_{max} - 1$  states are shown in Fig. 3. One can see, that now the effect of symmetry restoration is relatively small as compared to clearly dominant mean-field splitting. There is also an interesting difference between Sly4 and SkO forces. For the Sly4 force the isotonic and isotopic dependence of  $E(I_{max}) - E(I_{max} - 1)$  is very well reproduced but there is a constant offset between theoretical results and the data. This offset, after symmetry restoration, equals to  $\sim 455$  keV for the method A and to  $\sim 385$  keV for the method B. The opposite is true in the SkO case. This force does not reproduce details of isotopic and isotonic dependence, but reproduces quite well mean value of  $E(I_{max}) - E(I_{max} - 1)$ .

#### 4. Summary

We have shown that terminating states in  $A \sim 44$  mass region are excellent playground for testing and constraining various aspects of the nuclear EDF. In particular, unification of otherwise quite random coupling constants connected with

spin-fields to experimental data and slight reduction of SO strength allow to reach very good agreement with experimental data for maximum-spin  $I_{max}$  terminating states. Our study reveals that the SHF method cannot be directly applied to unfavored signature  $I_{max} - 1$  states. For these states the SHF solutions manifestly break rotational invariance at almost spherical shape. After identification of the underlying SSB mechanism we propose analytical symmetry restoration schemes for both  $[f_{7/2}^n]_{I_{max}-1}$  and  $[d_{3/2}^{-1}f_{7/2}^{n+1}]_{I_{max}-1}$  configurations. It is shown that for  $[f_{7/2}^n]_{I_{max}-1}$  the configuration mixing is absolutely necessary in order to reproduce empirical  $E(I_{max}) - E(I_{max} - 1)$  splitting. For  $[d_{3/2}^{-1}f_{7/2}^{n+1}]_{I_{max}-1}$  configuration on the other hand the splitting  $E(I_{max}) - E(I_{max} - 1)$  is dominated by mean-field itself and the symmetry restoration effect is relatively less important.

### 5. Acknowledgments

This work was supported in part the Polish Committee for Scientific Research (KBN) under contract No. 1 P03B 059 27 and by the Foundation for Polish Science (FNP).

### References

1. E. Caurier *et al.*, Rev. Mod. Phys. **77** (2005) 427.
2. M. Bender, P.-H. Heenen, and P.-G. Reinhard, Rev. Mod. Phys. **75** (2003) 121.
3. P. Hohenberg and W. Kohn, Phys. Rev. **136**, B864 (1964); W. Kohn and L.J. Sham, Phys. Rev. **140**, A1133 (1965); W. Kohn, Rev. Mod. Phys. **71**, 1253 (1998).
4. E. Perlińska *et al.*, Phys. Rev. C **69**, 014316 (2004).
5. T.H.R. Skyrme, Phil. Mag. **1** (1956) 1043; Nucl. Phys. **9** (1959) 615.
6. D. Vautherin and D.M. Brink, Phys. Rev. **C5** (1972) 626.
7. A.V. Afanasjev *et al.*, Phys. Rep. **322** (1999) 1.
8. W. Satula and R. Wyss, Rep. Prog. Phys. **68** (2005) 131.
9. G. Stoitcheva *et al.*, Phys. Rev. **C73** (2006) 061304(R).
10. H. Zduńczuk, W. Satula, and R. Wyss, Phys. Rev. **C71** (2005) 024305; Int. J. Mod. Phys. **E14** (2005) 451; W. Satula, R. Wyss, and H. Zduńczuk, Eur. Phys. J. A **25**, s01, (2005) 551..
11. E. Chabanat, *et al.*, Nucl. Phys. **A627** (1997) 710; **A635** (1998) 231.
12. P.-G. Reinhard *et al.*, Phys. Rev. **C60** (1999) 014316.
13. M. Beiner *et al.*, Nucl. Phys. **A238** (1975) 29.
14. B.A. Brown, Phys. Rev. **C58** (1998) 220.
15. F. Osterfeld, Rev. Mod. Phys. **64** (1992) 491.
16. M. Bender *et al.*, Phys. Rev. **C65** (2002) 054322.
17. S.G. Nilsson, Mat. Fys. Medd. Dan. Vid. Selsk. **29** (1955).
18. J. Dobaczewski, H. Flocard, and J. Treiner, Nucl. Phys. **A422** (1984) 103.
19. F. Tondeur *et al.*, Phys. Rev. **C62** (2000) 024308.
20. J. Bartel *et al.*, Nucl. Phys. **A386** (1982) 79.
21. M. Zalewski *et al.*, submitted to Phys. Rev. **C** (2006), LANL e-print nucl-th/0701020.